Stamped microbattery electrodes based on self-assembled M13 viruses

Ki Tae Nam[a], Ryan Wartena[a], Pil J. Yoo[b,1], Forrest W. Liau[a], Yun Jung Lee[a], Yet-Ming Chiang[a,2], Paula T. Hammond[b,2], and Angela M. Belcher[a,c,2]

Departments of [a]Materials Science and Engineering, [b]Chemical Engineering, and [c]Biological Engineering, Massachusetts Institute of Technology, Cambridge, MA 02139

Edited by Robert H. Austin, Princeton University, Princeton, NJ, and approved July 15, 2008 (received for review December 10, 2007)

The fabrication and spatial positioning of electrodes are becoming central issues in battery technology because of emerging needs for small scale power sources, including those embedded in flexible substrates and textiles. More generally, novel electrode positioning methods could enable the use of nanostructured electrodes and multidimensional architectures in new battery designs having improved electrochemical performance. Here, we demonstrate the synergistic use of biological and nonbiological assembly methods for fabricating and positioning small battery components that may enable high performance microbatteries with complex architectures. A self-assembled layer of virus-templated cobalt oxide nanowires serving as the active anode material in the battery anode was formed on top of microscale islands of polyelectrolyte multilayers serving as the battery electrolyte, and this assembly was stamped onto platinum microband current collectors. The resulting electrode arrays exhibit full electrochemical functionality. This versatile approach for fabricating and positioning electrodes may provide greater flexibility for implementing advanced battery designs such as those with interdigitated microelectrodes or 3D architectures.

biomineralization | self-assembly | battery | polyelectrolyte | nanoscience

Biological systems have developed unique abilities to grow and assemble nanostructures with an impressive degree of control, as is evident in biomineralization (1). Increased knowledge about the interface between biological molecules and inorganic materials has led to novel approaches in the design and fabrication of man-made devices (2–5). A variety of biomolecules including DNA (6, 7), peptides (8), and proteins have been functionalized, assembled into nanostructures, and implemented in electronic devices such as transistors, biosensors, memory devices, and battery electrodes. In our previous work, we have shown that the genetically engineered M13 virus serves as a model system to understand the interaction between peptides and inorganic materials (9) and can be used as a programmable molecular building block to template inorganic materials growth (10) and achieve self-assembly (11, 12). The filamentous M13 virus is ≈6.5 nm in diameter and 880 nm in length, with a genetically modifiable outer protein coat composed of 2,700 identical protein subunits (13). This makes the M13 virus a versatile toolkit for designing materials "from DNA sequences to functional devices." In addition, M13 libraries have been used extensively for biomolecules selection in biotechnology (13) and the M13 viruses have well established genetic modification protocols, and has had much of its structure (14) and biophysics unveiled (15, 16).

Biological approaches for electronic device fabrication are no longer in the early proof-of-concept stage but are now beginning to reveal new ways for improving device performance. For example, we recently reported that M13 viruses can be used in electrode fabrication to improve the storage characteristics and rate capability of a lithium ion battery (5). Through the addition of a small set of nucleotides into the viral DNA, specific functional groups with affinity for cobalt ions can be displayed on the viral major coat proteins. These engineered viruses were used to grow nanowires of cobalt oxide, which is representative of a new class of battery materials with much higher storage capacity than the carbon-based negative electrodes now used in lithium–ion batteries. In addition, we have also found that alternating electrostatic layer-by-layer assembly (LbL) can be used with the appropriate choice of polyelectrolytes to generate ultrathin multilayer films with ion transport properties that can act as solid state electrolytes (17–19). Given that the virus has a unique ability to self-assemble on top of polyelectrolyte multilayers via competitive charge interactions and/or enhanced polyelectrolyte chain mobility (20), we envisioned the possibility of using the virus to create a fully self-assembled battery. By using the toolkits of genetically engineered virus templates for biomineralization, multilayer assembly methods, and soft lithography, we report here the assembly and characterization of a stamped microbattery.

Despite ongoing research over several decades to improve battery performance, many challenges remain. From the design perspective, one of the key limitations is that, using presently available assembly techniques, less than half of the mass and volume of the battery is occupied by electrochemically active materials. This challenge is especially severe for smaller batteries (21): as battery size is reduced, the active fraction further diminishes. To increase energy density, and specific energy, it is highly desirable to reduce the relative amount of inactive supporting materials. The use of nanostructured battery materials represents another major direction of research in pursuit of improved performance (22–24). Furthermore, because electronics are becoming increasingly ubiquitous in new form factors ranging from flexible paper-thin cards to fibers to miniaturized implantable medical devices, there is a growing yet unmet demand for high-performance batteries in matching form factors. Although there has been significant research to integrate electronic nano devices (25–27), fewer investigations have focused on how to power these nano devices. Here, we present a versatile approach for fabricating and positioning small battery

This paper results from the Arthur M. Sackler Colloquium of the National Academy of Sciences, "Nanomaterials in Biology and Medicine: Promises and Perils," held April 10–11, 2007, at the National Academy of Sciences in Washington, DC. The complete program and audio files of most presentations are available on the NAS web site at www.nasonline.org/nanoprobes.

Author contributions: K.T.N., Y.J.L., Y.-M.C., P.T.H., and A.M.B. designed research; K.T.N., R.W., P.J.Y., and F.W.L. performed research; R.W., P.J.Y., Y.-M.C., and P.T.H. contributed new reagents/analytic tools; K.T.N., R.W., F.W.L., Y.J.L., Y.-M.C., P.T.H., and A.M.B. analyzed data; and K.T.N. and A.M.B. wrote the paper.

The authors declare no conflict of interest.

This article is a PNAS Direct Submission.

[1]Present address: Department of Chemical Engineering and SKKU Advanced Institute of Nanotechnology, Sungkyunkwan University, Suwon 440–746, Korea.

[2]To whom correspondence may be addressed. E-mail: ychiang@mit.edu, hammond@mit.edu, or belcher@mit.edu.

This article contains supporting information online at www.pnas.org/cgi/content/full/0711620105/DCSupplemental.

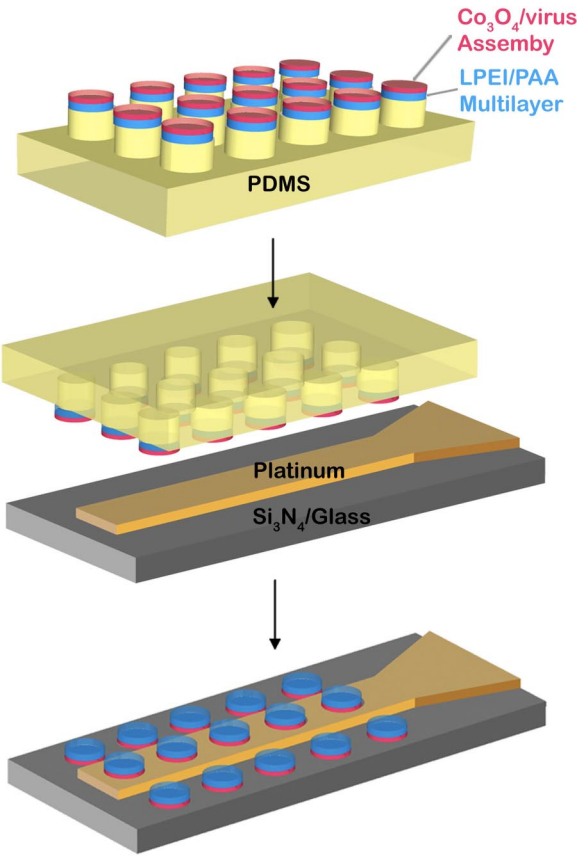

Fig. 1. Schematic procedure for constructing virus based microbattery electrodes. The virus-based cobalt oxide nanowires assembled on the polyelectrolyte multilayer were together stamped onto Pt microband current collectors.

components that may enable high performance microbatteries with complex architectures (e.g., interdigitated or 3D structures), and which could potentially be placed on flexible substrates (e.g., fibers or flex circuits). In this study, we combine biological assembly and microcontact printing technology to fabricate a hierarchically nanostructured battery anode, which is then positioned together with polymer-based solid electrolyte and microband current collectors onto a substrate.

Results and Discussion

The schematic procedure for constructing the microbattery electrode is shown in Fig. 1. A polydimethylsiloxane (PDMS) stamp of embossed microcylindrical patterns was fabricated by thermal-curing the prepolymer over a master pattern of photoresist. Two different cylindrical patterns were used to assess the versatility of this process: a 4-μm-diameter post with 5-μm center-to-center spacing (denoted as stamp pattern I) and an 8-μm-diameter post with 20-μm spacing (stamp pattern II). On the PDMS stamp pattern, polyelectrolyte multilayers were deposited by electrostatic layer-by-layer assembly techniques (28, 29) and served as the solid electrolyte and battery separator. Linear-polyethylenimine (LPEI, 25,000 M_r) was used as the polycationic building block and anionic polyacrylic acid (PAA, 90,000 M_r) was used as a counter charged polymer. Twelve bilayers of both LPEI and PAA were alternately deposited at pH 5. The height of the electrostatically deposited polymeric separator was 150 nm, as determined by ellipsometry. After polymer deposition, an M13 virus solution was dropcast onto the $(LPEI/PAA)_{12.5}$/PDMS. Tetraglutamate (EEEE-) was fused to the N terminus of each copy of the major coat p8 protein of the M13 virus by adding the corresponding nucleotides to gene 8. By dipping the assembled viruses in cobalt oxide precursor solution, planar micropatterns of cobalt oxide nanowires corresponding to the stamped patterns were grown on the polyelectrolyte multilayers. These multilayers act as a solid electrolyte and separator for lithium ion transport (30). The microbattery electrodes comprising the virus-templated cobalt oxide anodes and solid polymeric electrolyte were transferred onto four lines of platinum microband current collectors (Abtech Scientific) by using an adaptation of the multilayer transfer method (29). The stamp pattern I (4-μm-diameter cylinders) was transferred onto microbands of 10-μm width, 10-μm pitch, and 3-mm length; and stamp pattern II (8-μm-diameter cylinders) was transferred onto microbands of 20-μm width, 20-μm pitch, and 3-mm length. During the pattern transfer, a slight pressure of a few bars was applied to ensure conformal contact between the PDMS mold and the line-patterned platinum electrode. For more efficient electron transfer, the platinum electrode was lightly treated with air plasma for 20 sec to increase the surface energy and rinsed with a few drops of water. Successful pattern transfers were achieved irrespective of the pattern size or the width of the platinum microbands.

Fig. 2*A* is an atomic force microscopic (AFM) image of the microbattery anode and solid electrolyte assembled on a PDMS stamp before pattern transfer. The stacking order from top to bottom is cobalt oxide/virus/(LPEI/PAA)/PDMS. The thicker deposition of polymer layers near the edges of the patterns observed was presumably from localized solution condensation during the repeated dipping and washing steps of the layer-by-layer deposition. 2D assemblies of viruses on top of the poly-

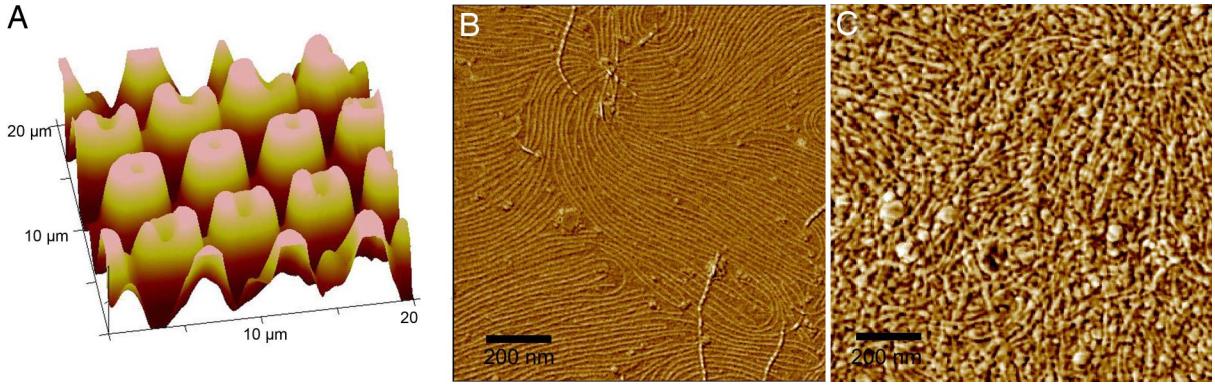

Fig. 2. Virus-based microbattery electrodes on PDMS stamp. (*A*) Height-mode AFM images of virus-based microbattery electrode on PDMS stamp (4-μm-diameter cylinders, pattern I) measured before the transfer to the current collectors. Z range is 2 μm. (*B*) Phase-mode AFM image of virus assembly before cobalt oxide growth. (*C*) AFM image of virus based microelectrode after cobalt oxide growth.

electrolyte multilayers are shown in Fig. 2*B*. The virus ordering is a result of a combination of liquid crystalline repulsive interactions between the viruses and interdiffusion between LPEI and PAA. The enhanced surface mobility of the polyelectrolytes gained from a polymeric interdiffusion process can augment the surface mobility of electrostatically bound M13 viruses on top of the polyelectrolyte multilayers, eventually leading to the formation of a 2D liquid crystalline assembly of viruses (20). Fig. 2*C* shows the surface morphology after growth of cobalt oxide nanowires on the virus-assembled monolayer. Nanoscale cobalt oxide is representative of a promising class of lithium–ion battery electrodes that have very high reversible capacity arising from displacement reactions occurring at the nanoscale (31). This virus-mediated charge interaction assembly method is capable of achieving high-nanostructure packing density of the active materials while maintaining the structural integrity of the assembled nanostructures (5). In contrast, conventional methods for depositing nanoparticles or nanowires on multilayers typically result in 3D network structures of low packing density. The 2D structures presented here show promise for the high-density assembly of nanowires for applications including microbatteries and other microdevices. Furthermore, if supplemented by various adsorption and microfluidics techniques, this method could produce oriented, close-packed viral systems for templating structures in three dimensions.

For electrochemical characterization, micropads of electrochemically active anode material and polymer solid electrolyte were transferred to a platinum line pattern. Fig. 3*A* shows microbattery pattern I (without cathode) on the platinum microband current collectors. This current collector is composed of four microbands that broaden at one end to accommodate external electrical contact as shown in Fig. 3*A Lower*.

The optical image in Fig. 3*B* clearly shows the arrangement of the microbatteries. On average, two columns of 4-μm-diameter microbatteries were placed across one platinum line for pattern I, and one column of 8-μm-diameter was placed across one platinum line for pattern II. In Fig. 3*B*, the rectangular outline shows the exposed active areas; the region outside the box is passivated by a deposition of insulating silicon dioxide. These microbattery electrodes could also be placed uniformly over a larger target area. Furthermore, this method is potentially applicable to the assembly of other devices requiring small-area charge storage or sensing components. In particular, the additional stamping of cathodes onto the same substrate as the anodes could produce batteries with interdigitated electrode architectures. Closer observation of the microelectrodes (Fig. 3*C*) by SEM also validates the uniformity of the transferred microelectrode over a large-length scale. One interesting feature visible by SEM is the wrinkle formation on the microelectrode. The wavelength of the wrinkling is ≈300 nm. We speculate that the wrinkling is driven by the swelling and evaporation of solvent in the polyelectrolyte multilayers.

Detailed electrochemical analysis was conducted on the 8-μm-diameter composite anodes and the polyelectrolyte printed from stamp pattern II onto 20-μm-wide 3-mm-long platinum microband current collectors. As shown in Fig. 3*A*, all four platinum microbands were jointed to a single external copper contact. The assembled sample was tested against a counterelectrode made of 1-cm^2 lithium foil (FMC Lithium) mounted on copper foil (20-μm thick, Alfa Aesar). The test cell was assembled with a porous polymer separator (20-μm thick, polyethylene-polypropylene-polyethylene, Tonen) separating the two electrodes. The stacked cell was heat-sealed in a metallized polymer bag, filled with liquid electrolyte (battery-grade electrolyte, 1.3M $LiPF_6$ in propylene carbonate/ethylene carbonate/dimethylene carbonate, Ferro) and allowed to reach equilibrium before electrochemical testing was initiated.

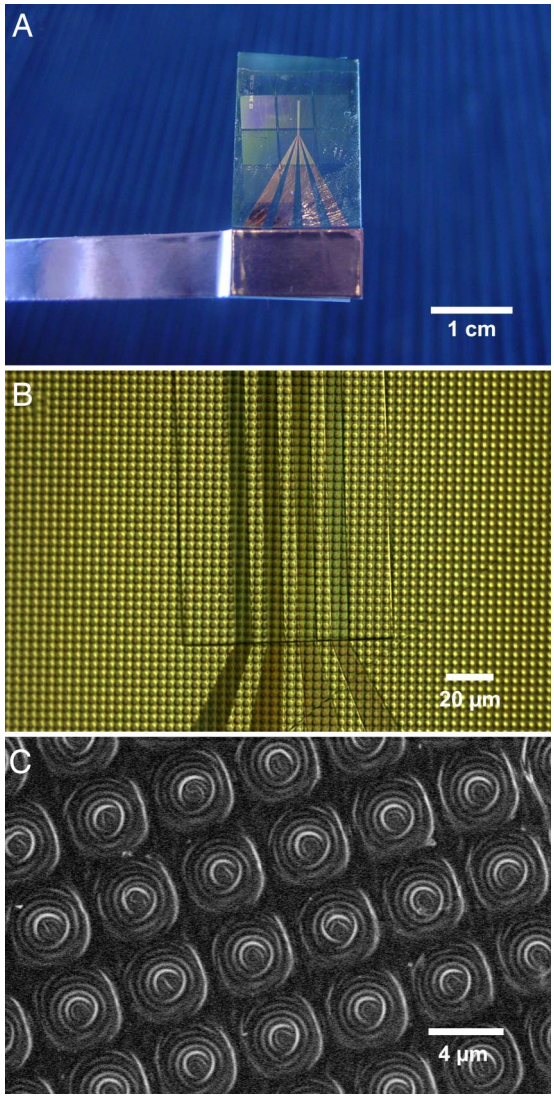

Fig. 3. Self-assembled and stamped microbattery electrode based on the M13 viruses. (*A*) Image of microbatteries on the Pt current collector. (*B*) Optical microscopy image of the microbattery electrode (4-μm diameter) on four Pt microband current collectors (10-μm width). (*C*) SEM image of the stamped microbattery electrode.

Using a Solartron 1287 potentiostat with electrochemical interface (Solartron Analytical), the assembled cells were galvanostically cycled between 3.0 and 0.1 V at various currents from 255 to 26 nA. In each cycle, the cell was allowed to rest for 2 hr after charging to observe the polarization relaxation and to allow equilibration at a stable open-circuit voltage. The cell was then galvanostatically discharged to 0.1 V at various currents to determine the microelectrode's charge storage capacity and rate performance (Fig. 4*C*). Voltage/capacity curves (Fig. 4*A*) for the microelectrode cell show similar behavior to those for Co_3O_4 nanoparticles produced by other methods (31). At the slowest charging rate (26 nA), the microelectrode array showed discharge capacity ranging from 375 to 460 nAh. In previous work with platinum current collectors, we found that the platinum itself can contribute a limited amount of lithium storage capacity because of formation of intermetallic compounds such $LiPt_7$, $LiPt_2$, LiPt, and Li_2Pt, especially at slow charging rates. In the current geometry, the four platinum microbands are estimated to contribute 41 nAh capacity or ≈10% of the total capacity measured at the slowest charging rate. The gravimetric specific

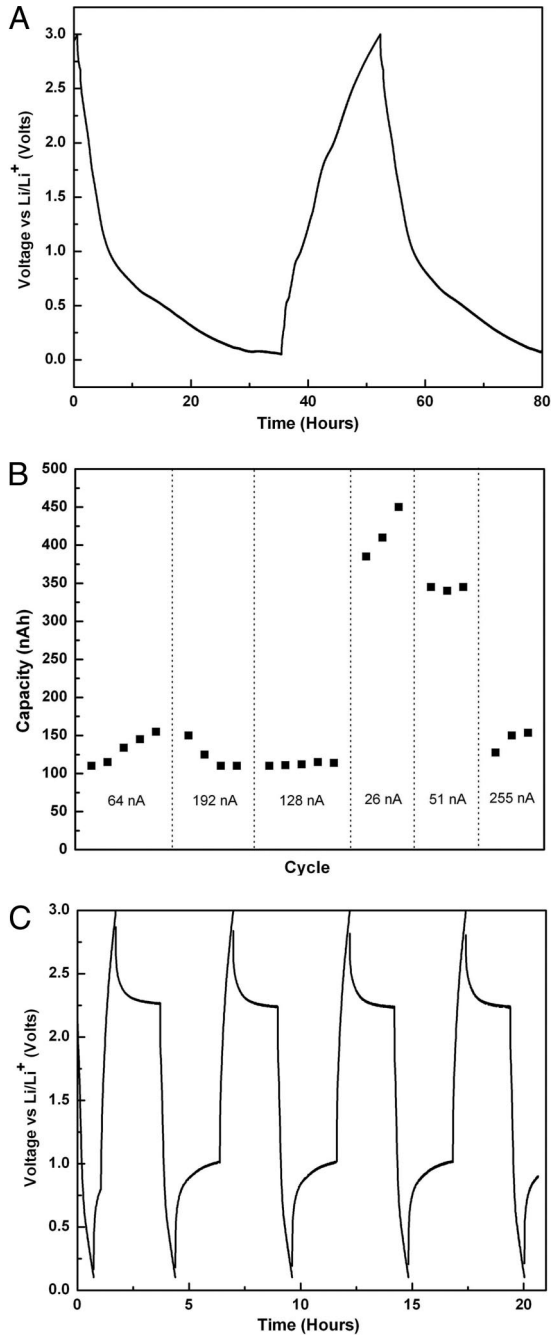

Fig. 4. Electrochemical testing of stamped microbatteries based on the M13 viruses (*A*) Charge-discharge curve for a virus assembled cobalt oxide microelectrode tested vs. Li/Li^+, cell cycled between 3 and 0.01 V at a rate of 26 nA. (*B*) Capacity vs. cycle number for the same cell at six different charging currents. (*C*) Charge-discharge curve at a rate of 255 nA. A 2-h rest after charging and discharging in each cycle allows for cell equilibration. Stable cycling of the microbattery is exhibited.

capacity (mAh/g) was not calculated in these experiments because of the difficulty of determining the exact mass of cobalt oxide in the microelectrode. However, we assume that the specific capacity of the virus-based cobalt oxide nanowires should be similar to our previous data (5) on a 2D planar assembly, because these nanowires were synthesized by using the same synthesis method. Because there are 150 microelectrodes on each platinum microband of 20-μm width, we estimate that each microelectrode can have a storage capacity between 625 and 766 pAh.

Fig. 4*B* is a summary plot of the discharge capacity (nAh) of the microelectrode assembly consisting of the composite anodes and polyelectrolyte on the microbands, as a function of discharge rate. The capacity ranges from 380 to 460 nAh at low discharge current (26 nA) to 100–150 nAh at high discharge current (255 nA). Discharge currents higher than 64 nA led to a decrease of the capacity to 25% of the maximum value but with no further decreases with increasing current. We used SEM to analyze the mechanical stability of our microelectrode after 25 cycles at various charging. The analysis shows that the microbattery electrodes are structurally stable and do not fall apart from the Pt electrodes after cycling [see supporting information (SI) Fig. S1].

Fig. 4*C* shows the cycling stability of the virus-based microbattery electrode. The stable open-circuit voltage after each charge or discharge cycle and the consistent open circuit voltage values between cycles, shows that the electrochemical reaction of Li with the Co_3O_4 nanowires is stable and reversible, as was the case for these nanowires tested in a previous configuration. More detailed graphs of the charging (0.7–1.8 h) and discharging curve (3.6–4.4 h) of Fig. 4*C* (Fig. S2) demonstrate that the microbattery electrodes exhibit a similar charging/discharging curve as that of Co_3O_4 nanoparticles produced by other methods, even at a high charging rate of 255 nA. Direct comparison to other microbattery assembly approaches, such as thin-film vapor deposition (32), laser direct-write printing (33), and sol gel printing (34), cannot be made easily because of differences in the electrode materials tested and the electrode geometries.

The microbattery electrodes can be easily transferred to a variety of substrates by stamping. The microcontact printing technique demonstrated in this study could enable economical small-scale patterning of viruses and virus-templated nanostructures on a variety of substrates with a vast range of chemical functionalities. Until now, microcontact printing techniques have been used solely for fabricating functional electronic devices, complex optical devices, and biological devices (35, 36). This work demonstrates the use of microcontact printing to position microbattery electrodes formed by virus-based assembly.

Conclusion

The approach presented here for combining polymer electrostatic assembly techniques and biological self-assembly at multiple lengthscales may be used to construct small-scale power sources embedded in various system structures. Here, we demonstrated that traditional soft lithography technology and an understanding of the interface between polymers, viruses and inorganic materials can be combined for the fabrication and positioning of microbattery electrodes. Furthermore, such microbattery electrodes can be easily stamped on a variety of rigid or flexible substrates to construct microbatteries with stable, reliable performance. This versatile approach incorporating both biological and nonbiological assembly strategies may provide greater flexibility for implementing advanced battery designs such as those with interdigitated microelectrodes or 3D architectures. Cathode materials are currently being investigated for a fully self-assembled microbattery. We anticipate that further advances in biotemplating, self-assembly, and polymeric nanopattern designs will provide additional flexibility in the design of novel battery architectures.

Methods

Layer-by-Layer Deposition of Polyelectrolyte Multilayers. LPEI (25,000 and 250,000 M_r) (Polysciences) and PAA (90,000 M_r, 25% aqueous solution) (Polysciences) were prepared as 0.02-M solutions based on the repeat-unit molecular weight in Milli-Q water. The pH of the LPEI and PAA solutions was adjusted to 5.0. LPEI/PAA multilayer thin films were deposited on PDMS mold by conventional LbL method by using an HMS programmable slide stainer (Zeiss).

Virus-Enabled Synthesis and Assembly of Microbattery Electrode. Tetraglutamate (EEEE-) was fused to the N terminus of each copy of the major coat p8 protein of M13 viruses through adding the corresponding nucleotides to gene 8, as described (5). The genetically engineered M13 viruses were amplified by using *Escherichia coli* bacteria medium. The viruses were diluted in a water to have a concentration of 10^{10} phages/ml, and the pH was adjusted to 5.0 by adding 0.01 M HCl. Then, 1 ml of the virus solution was dropped on LPEI/PAA film (2×4 cm). After incubation for 30 min, the virus-assembled film was rinsed with Milli-Q water and dried by blowing with nitrogen. The virus-assembled LPEI/PAA film on PDMS pattern was incubated in 15-ml aqueous solution of cobalt chloride (1 mM) for 15 min. Then 15 ml of $NaBH_4$ (5 mM) was added to nucleate cobalt on the M13 virus templates. The incubation of virus templated cobalt in aqueous solution resulted in the spontaneous oxidation into cobalt oxide.

Microscopy Analysis. The phase or height image of the assembled and transferred microbatteries was analyzed by using AFM in tapping mode (Dimension 3000, Veeco Instruments). Transferred microbatteries on the platinum microbands were observed by using an Olympus microscope (IX51).

ACKNOWLEDGMENTS. We thank Jifa Qi for the SEM imaging in Fig. 3C. This work was supported by the Army Research Office Institute of Collaborative Biotechnologies (ICB), the Army Research Office Institute of Soldier Nanotechnologies (ISN), and the David and Lucille Packard Foundation.

1. Mann S (1996) *Biomimetic Materials Chemistry* (VCH, New York).
2. Carette N, *et al.* (2007) A virus-based biocatalyst. *Nat Nanotechnol* 2:226–229.
3. Douglas T, Young M (2006) Viruses: Making friends with old foes. *Science* 312:873–875.
4. Dujardin E, Peet C, Stubbs G, Culver JN, Mann S (2003) Organization of metallic nanoparticles using tobacco mosaic virus templates. *Nano Lett* 3:413–417.
5. Nam KT, *et al.* (2006) Virus-enabled synthesis and assembly of nanowires for lithium ion battery electrodes. *Science* 312:885–888.
6. Braun E, Eichen Y, Sivan U, Ben-Yoseph G (1998) DNA-templated assembly and electrode attachment of a conducting silver wire. *Nature* 391:775–778.
7. Seeman NC, Lukeman PS (2005) Nucleic acid nanostructures: Bottom-up control of geometry on the nanoscale. *Rep Prog Phys* 68:237–270.
8. Zhang SG (2003) Fabrication of novel biomaterials through molecular self-assembly. *Nat Biotechnol* 21:1171–1178.
9. Whaley SR, English DS, Hu EL, Barbara PF, Belcher AM (2000) Selection of peptides with semiconductor binding specificity for directed nanocrystal assembly. *Nature* 405:665–668.
10. Mao CB, *et al.* (2004) Virus-based toolkit for the directed synthesis of magnetic and semiconducting nanowires. *Science* 303:213–217.
11. Nam KT, Peelle BR, Lee SW, Belcher AM (2004) Genetically driven assembly of nanorings based on the M13 virus. *Nano Lett* 4:23–27.
12. Lee SW, Mao CB, Flynn CE, Belcher AM (2002) Ordering of quantum dots using genetically engineered viruses. *Science* 296:892–895.
13. Barbas CF (2001) *in Phage Display : A Laboratory Manual* (Cold Spring Harbor Lab Press, Cold Spring Harbor, NY).
14. Marvin DA, Welsh LC, Symmons MF, Scott WRP, Straus SK (2006) Molecular structure of fd (f1, M13) filamentous bacteriophage refined with respect to X-ray fibre diffraction and solid-state NMR data supports specific models of phage assembly at the bacterial membrane. *J Mol Biol* 355:294–309.
15. Khalil AS, *et al.* (2007) Single M13 bacteriophage tethering and stretching. *Proc Natl Acad Sci USA* 104:4892–4897.
16. Dogic Z, Fraden S (2006) Ordered phases of filamentous viruses. *Curr Opin Colloid Interface Sci* 11:47–55.
17. DeLongchamp DM, Kastantin M, Hammond PT (2003) High-contrast electrochromism from layer-by-layer polymer films. *Chem Mater* 15:1575–1586.
18. Lowman GM, Hammond PT (2005) Solid-state dye-sensitized solar cells combining a porous TiO2 film and a layer-by-layer composite electrolyte. *Small* 1:1070–1073.
19. Lowman GM, Tokuhisa H, Lutkenhaus JL, Hammond PT (2004) Novel solid-state polymer electrolyte consisting of a porous layer-by-layer polyelectrolyte thin film and oligoethylene glycol. *Langmuir* 20:9791–9795.
20. Yoo PJ, *et al.* (2006) Spontaneous assembly of viruses on multilayered polymer surfaces. *Nat Mater* 5:234–240.
21. Cho YK, Wartena R, Tobias SM, Chiang YM (2007) Self-assembling colloidal-scale devices: Selecting and using short-range surface forces between conductive solids. *Adv Funct Mater* 17:379–389.
22. Arico AS, Bruce P, Scrosati B, Tarascon JM, Van Schalkwijk W (2005) Nanostructured materials for advanced energy conversion and storage devices. *Nat Mater* 4:366–377.
23. Meethong N, Huang HYS, Speakman SA, Carter WC, Chiang YM (2007) Strain accommodation during phase transformations in olivine-based cathodes as a materials selection criterion for high-power rechargeable batteries. *Adv Funct Mater* 17:1115–1123.
24. Chung SY, Bloking JT, Chiang YM (2002) Electronically conductive phospho-olivines as lithium storage electrodes. *Nat Mater* 1:123–128.
25. Kang SJ, *et al.* (2007) High-performance electronics using dense, perfectly aligned arrays of single-walled carbon nanotubes. *Nat Nanotechnol* 2:230–236.
26. Yu GH, Cao AY, Lieber CM (2007) Large-area blown bubble films of aligned nanowires and carbon nanotubes. *Nat Nanotechnol* 2:372–377.
27. Huang Y, *et al.* (2001) Logic gates and computation from assembled nanowire building blocks. *Science* 294:1313–1317.
28. Hammond PT (2004) Form and function in multilayer assembly: New applications at the nanoscale. *Adv Mater* 16:1271–1293.
29. Park J, Hammond PT (2004) Multilayer transfer printing for polyelectrolyte multilayer patterning: Direct transfer of layer-by-layer assembled micropatterned thin films. *Adv Mater* 16:520–525.
30. Lutkenhaus JL, Hammond PT (2007) Electrochemically enabled polyelectrolyte multilayer devices: From fuel cells to sensors. *Soft Matter* 3:804–816.
31. Poizot P, Laruelle S, Grugeon S, Dupont L, Tarascon JM (2000) Nano-sized transition-metaloxides as negative-electrode materials for lithium-ion batteries. *Nature* 407:496–499.
32. Bates JB, Dudney NJ, Neudecker B, Ueda A, Evans CD (2000) Thin-film lithium and lithium-ion batteries. *Solid State Ionics* 135:33–45.
33. Wartena R, Curtright AE, Arnold CB, Pique A, Swider-Lyons KE (2004) Li-ion microbatteries generated by a laser direct-write method. *J Power Sources* 126:193–202.
34. Dokko K, *et al.* (2007) Sol-gel fabrication of lithium-ion microarray battery. *Electrochem Commun* 9:857–862.
35. Menard E, *et al.* (2007) Micro- and nanopatterning techniques for organic electronic and optoelectronic systems. *Chem Rev* 107:1117–1160.
36. Ahn JH, *et al.* (2006) Heterogeneous three-dimensional electronics by use of printed semiconductor nanomaterials. *Science* 314:1754–1757.